STARE: A new detector array for exploring the breakup reaction mechanisms induced by weakly bound nuclei[*]

Y.S. Wu,[1] G.L. Zhang,[1, †] C.J. Lin,[2, ‡] N.R. Ma,[2] L. Yang,[2] G.X. Zhang,[3] S. P. Hu,[4, 5] H.Q. Zhang,[2] M. Mazzocco,[6, 7] Y.J. Yao,[1] Z.W. Jiao,[1] M.L. Wang,[1] X.D. Su,[1] H.B. Lv,[1] and K. Dong[1]

[1]*School of Physics, Beihang University, 100191 Beijing, China*
[2]*China Institute of Atomic Energy, Beijing 102413, China*
[3]*Sino-French Institute of Nuclear Engineering and Technology, Sun Yat-Sen University, Zhuhai 519082, China*
[4]*Institute for Advanced Study in Nuclear Energy & Safety, Shenzhen University, China*
[5]*Shenzhen Key Laboratory of Research and Manufacture of High Purity Germanium Materials and Detectors, Shenzhen University, 518060*
[6]*Dipartimento di Fisica e Astronomia, Università di Padova, Padova 35131, Italy*
[7]*Istituto Nazionale di Fisica Nucleare, Sezione di Padova, Padova 35131, Italy*

A new detector array with a large solid angle coverage for coincidence measurement of charged fragments was developed to study the breakup reaction mechanisms of weakly bound nuclear systems at energies around the Coulomb barrier. The array has been used for exploring the breakup reaction mechanisms of ^{6,7}Li + ^{209}Bi systems at E_{beam} = 30, 40, 47 MeV, showing good performances of particle identification and complete kinematic measurements. Based on this, different breakup modes are distinguished clearly and some new breakup modes are discovered, such as ^{7}Li $\rightarrow \alpha + t$ breakup mode in ^{6}Li + ^{209}Bi system and ^{7}Li $\rightarrow$ ^{6}He + p breakup mode in ^{7}Li + ^{209}Bi system. It is shown that this array can be also used to explore other breakup reaction mechanisms induced by weakly bound nuclei.

Keywords: Detector array, Coincidence measurement, Breakup reaction,Weakly bound nuclei

I. INTRODUCTION

Nuclear reactions at energies near the Coulomb barrier are effective ways to study the interaction between nuclear structure and dynamics. As more exotic weakly bound nuclei become accessible at new accelerator facilities, the measurement of reaction cross sections for weakly bound nuclear systems at sub-barrier energies is of large interest [1, 2]. At present, it is found that in reactions involving these weakly bound nuclei, compared to theoretical calculations and tightly bound nuclei, the complete fusion has a significant suppression at energies above the Coulomb barrier and a remarkable enhancement at energies below the Coulomb barrier [3–9]. In order to investigate the breakup effects of weakly bound nuclei on the suppression of the complete fusion cross section, the study of the breakup reaction and mechanism of weakly bound nuclei has a crucial importance [10–13].

In comparison with radioactive ion beam (RIB), the beam intensities of stable weakly bound nuclei such as ^{6,7}Li and ^{9}Be are orders of magnitude higher [14]. A number of silicon detector arrays, such as GLORIA [15], EXPADES [16], BALiN [17], have recently been built to study the breakup mechanism induced by those stable weakly bound nuclei. Along with the identification of some breakup modes, the breakup effect of those nuclei on the fusion process has been preliminarily studied. However, due to the limited coverage angle of the previously mentioned detector arrays and the complexity of breakup modes, it is challenging to detect rare breakup events and to obtain the angular distribution of different breakup products.

In view of this fact, a new **S**ilicon **T**elescopic **A**rray for **R**eactions induced by **E**xotic nuclei (STARE), designed by China Institute of Atomic Energy (CIAE), is employed for coincidence measurement of charged fragments induced by weakly bound nuclei at energies around the Coulomb barrier. The coincidence measurement of ^{6,7}Li + ^{209}Bi at E_{beam} = 30, 40, 47 MeV was successfully carried out in CIAE by STARE. In this paper, the innovation features and performance of STARE, as well as the methods and preliminary results in the data analysis will be described in detail.
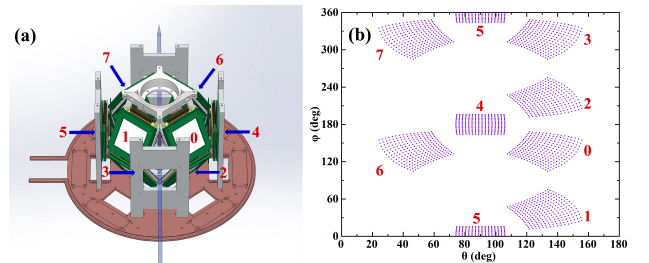
II. DESCRIPTION OF THE ARRAY

Fig. 1. (Color online) (a) The arrangement of the detector array of eight telescopes with respect to the beam direction (arrow from bottom to top). (b) Angular coverage of detector array, pixel separation in each DSSD is exaggerated for clarity.

STARE consists of eight telescope units as shown in Fig. 1(a). Each telescope unit consists of (i) a double-sided

silicon strip detector (DSSD) with a thickness of 40 μm for backward angles and 60 μm for forward angles, and (ii) a quadrant silicon detector (QSD) with a thickness of 1000 μm. Additional QSD with a thickness of 300 μm could be inserted between the DSSD and the 1000 μm thick QSD at forward angles. Some brief description of this detector array is given in Refs. [18, 19]. The eight telescope units surrounding the target were installed on a designed frame produced by 3D printing, which makes the array lighter and easy to be carried. The relative positions of the telescope units and the target are summarized in Table. 1. As shown in Fig. 1(b), the array covers polar angles θ_{lab} from 25° to 155°, and spans 301° in azimuthal angle, occupying 26.8% of the 4π sr. A larger number of telescope units provides larger solid angle coverage, greatly improving the coincidence detection efficiency compared with previous experiments [20–22].

Table 1. The information of different telescope units.

Unit No.	Distance between unit and target (mm)	The angle of the center of each unit (θ, ϕ)
0	70	132.1°, 139.2°
1	70	132.1°, 40.8°
2	70	132.1°, 220.8°
3	70	132.1°, 319.2°
4	82	90°, 180°
5	82	90°, 0°
6	70	47.9°, 139.2°
7	70	47.9°, 319.2°

A mylar foil with a thickness of 0.5 μm was installed in front of the telescope to stop low-energy electrons. As illustrated in Fig. 1(a), the compact structure makes possible to install the mylar foil and silicon detectors as close as possible each other with the lowest energy loss and angular straggling. Moreover, the integrated preamplifiers designed by CIAE [23] are installed in close proximity to the detectors and positioned in the target chamber to reduce noise. To ensure the stable operation of the preamplifiers, a cooling system is employed to dissipate the heat of the electronics and to reduce the detector leakage current. Specifically, two brass rings are mounted on top and below of the detector array, and all preamplifiers are fixed to these brass rings. During experiments, brass rings are cooled using a dedicated cooling system, providing a stable and low-temperature operating environment for the preamplifiers. A specific photo is shown in Fig. 2.

Silicon detectors are widely used nowadays, because of their high detection efficiency and good energy resolution [24]. In STARE, the kinetic energy of the particles was taken from the energy signal of the pixel of DSSDs, with resolution of 100-150 keV FWHM for $\sim$5 MeV α sources. To provide supporting evidence, Fig. 3 presents the energy spectra of the α sources measured by DSSDs of 40, 60 μm. The energy resolution of the peak corresponding to ^{239}Pu is determined to be $\sim$2.0%, 1.8%, respectively. Fig. 1(b) shows the scattering angles of the centers of all DSSD pixels. We can infer that the angular resolution in the central region of each pixel of DSSDs is approximately $\pm$1.5°, with improved
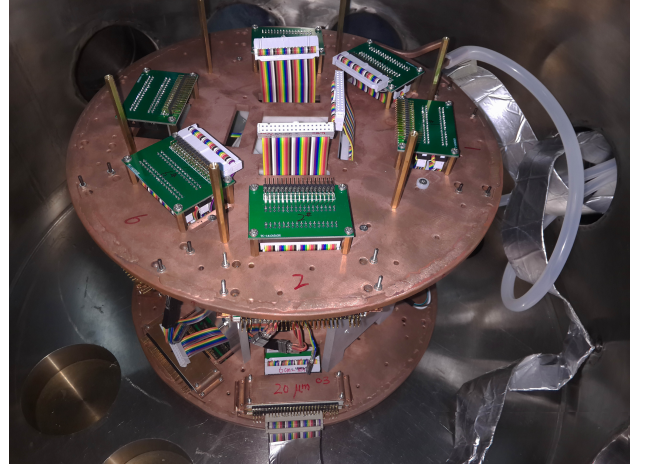

Fig. 2. (Color online) Photo of the detector array with preamplifiers and cooling rings.

resolution observed in the peripheral regions of the detector telescopes in the laboratory frame. Complete kinematic measurements can be carried out with good energy and angular resolutions, which are meaningful for reproducing the breakup process.
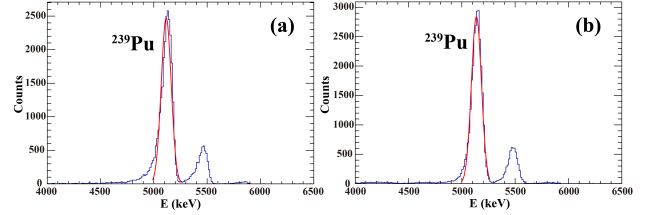

Fig. 3. (Color online) The energy spectra of the α sources measured by DSSDs of STARE. (a) from 40 μm DSSD; (b) from 60 μm DSSD.

III. EXPERIMENT

The coincidence measurements with beams of ^{6,7}Li were conducted at the HI-13 tandem accelerator of the CIAE. The beam energies at the center of the ^{209}Bi target (210 μg/cm^2 thick self-supporting) were about E_{beam} = 30, 40, 47 MeV. A collimator with a 3 mm diameter was positioned 30 cm upstream of the target, aligned along the beam axis, to precisely define the beam spot size and position. The target was fixed in the center of STARE with a normal angle of 70° relative to the beam line, to minimize the dead area caused by the target frame. Four silicon detectors were installed at a distance of 250 mm from the center of the target for beam monitoring. To minimize the data collection rate during breakup measurements, the data were recorded when at least two pixels of the whole detector array were hit by particles called multi-hit trigger mode.

IV. DATA ANALYSIS

A. Energy calibration

The energy calibration of the DSSDs was carried out by using two α sources (^{239}Pu, ^{241}Am) and the α particles decayed from the products of fusion reactions. Additionally, the energy calibrations of the QSDs were performed by evaluating the deposited energies of charged particles within the QSDs. This was achieved by subtracting the measured energy loss in the DSSDs from the expected particle energy, as determined through calculations using the reference for LISE++ [25]. In the experiment, the coordinate location of the DSSDs pixels can be used to determine the scattering angle of the charged particles detected by the detectors. A typical energy-calibrated single spectrum for ^{7}Li + ^{209}Bi measured at E_{beam} = 40 MeV is presented in Fig. 4 and shows elastic scattering events at ~36 MeV. For reactions in normal kinematics that produce two nuclei in the final state, such as elastic scattering or transfer, the energy of the projectile-like nucleus decreases monotonically with θ. The α lines between 5 and 10 MeV visible in Fig. 4, with energies independent of angle, originate from the evaporation residues formed following complete fusion (CF) and incomplete fusion (ICF).
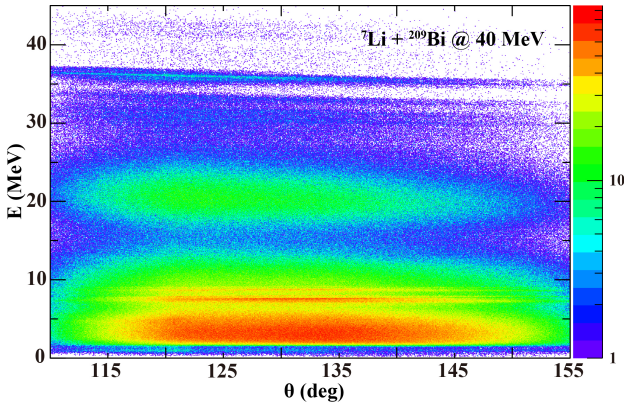

Fig. 4. (Color online) Energy-calibrated single spectrum for ^{7}Li + ^{209}Bi measured at E_{beam} = 40 MeV and displayed across the angular coverage of No.0-3 telescope units.

B. Removal of spurious events

According to the principle of DSSDs, we use the energy signals output from both sides of DSSDs (marked E_{loss1}, E_{loss2}, respectively) to select the correct events. As shown in Fig. 5(a), considering the statistics of events and the proportion of accidental coincidences, we pick up the events with E_{loss1} - E_{loss2} distributed within the σ (~100 keV) widening range as correct events. The two-dimensional spectrum E_{loss1} vs. E_{loss2} after screening is shown in Fig. 5(b). During the experiment, a large number of particles hits the interstrips of the DSSDs leading to a non-negligible number of accidental coincidence events (~3%). The two-dimensional spectrum of particles depositing energy in adjacent strips of the same DSSD is illustrated in Fig. 5(c). Various sources of accidental events can be observed, labeled in different regions. Region 1 represents that both particles are elastic scattered particles, regions 2 and 3 represent that one of the particles is elastic scattered and the other is a random particle in the adjacent strip, regions 4, 5, and 6 may be caused by particles hitting the inter-strips, but the charge is not completely collected by the adjacent strips. The regions explain various sources of accidental events, which will be removed for the next data analysis.
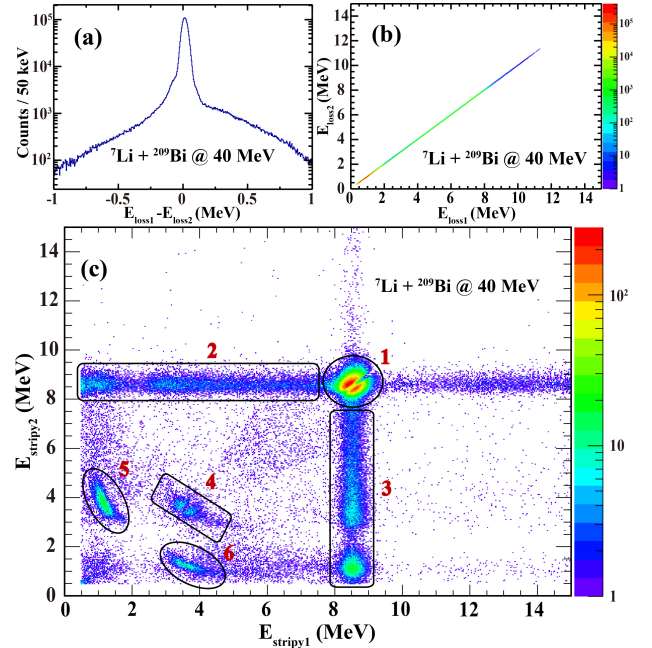

Fig. 5. (Color online) Example of No.6 telescope unit to demonstrate accidental events removal from ^{7}Li + ^{209}Bi at E_{beam} = 40 MeV. (a) The single energy spectrum of the difference in energy loss between the two sides of DSSD. (b) The two-dimensional energy spectrum E_{loss1} vs. E_{loss2} of the two sides of DSSD after screening based on (a). (c) Particle energy deposition on adjacent silicon strips in the same side of DSSD.

Typical two-dimensional particle identification spectra obtained from the same telescope unit are shown in Fig. 6. Owing to the excellent energy resolution of detectors and statistics, the different masses (A = 1–7) and charges (Z = 1–3) produced by different reaction channels can be identified clearly. Especially, the ^{3}He and ^{6}He bands can be observed in the experimental data of ^{6,7}Li, which provides the possibility for the observation of new breakup modes. In Fig. 6(a), ^{7}Li band can be observed. It is evident that ^{6}Li picked up one neutron from the target, thus 1n-pickup process induced by ^{6}Li can be occurred. In Fig. 6(b), ^{6}Li band can be observed. It occurs from 1n-stripping of ^{7}Li. It is shown that 1n-stripping process is populated in the reactions of ^{7}Li. The other light particles were analyzed in sections below.
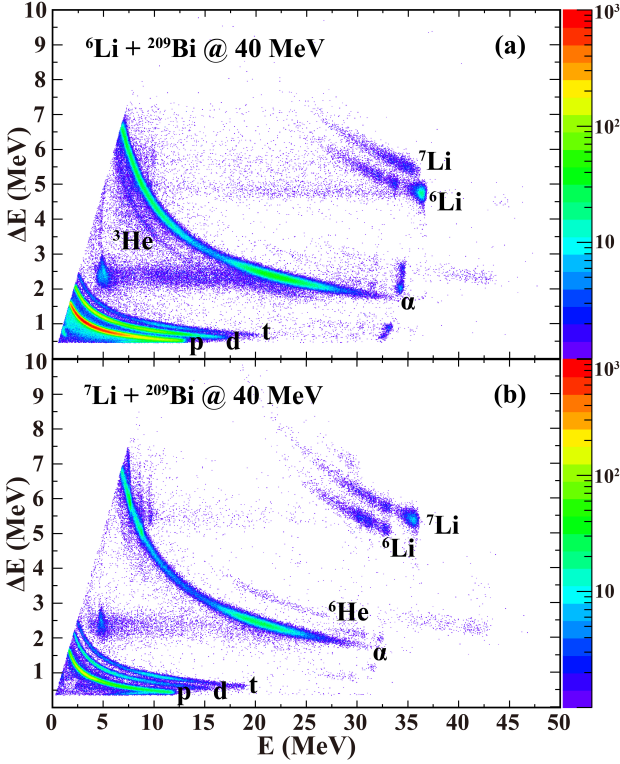
Fig. 6. (Color online) Calibrated two-dimensional ΔE-E particle identification spectra by No.2 telescope unit which covers an angular range from $110°$ to $155°$. (a) for ^{6}Li + ^{209}Bi at E_{beam} = 40 MeV; (b) for ^{7}Li + ^{209}Bi at E_{beam} = 40 MeV.

C. Identification of breakup modes

During a breakup process, momentum conservation dictates that the total momentum of the fragments should remain zero in the center of mass frame of the projectile-like nucleus. Thus, fragments must travel opposite directions in the center of mass frame, but may be emitted in any direction. As a result, we can filter out α particles from the breakup process as shown in Fig. 7(a) from ^{6}Li + ^{209}Bi at E_{beam} = 40 MeV, when a continuous distribution of energies with maximum and minimum energy are given by:

$$E_{min,max} = \frac{m_1}{m_1 + m_2}\left(E_p + \frac{m_2}{m_1}Q_{BU} \pm 2\sqrt{\frac{m_2}{m_1}Q_{BU}E_p}\right) \tag{1}$$

E_p is the projectile-like fragment energy prior to breakup, m_i the masses of the breakup fragments and Q_{BU} is the Q-value for the breakup process. Fig. 7(b) shows the current particle multiplicity (the number of particles contained in a coincidence event). We can observe that inclusive elastic scattering or transfer events still account for the majority, and the rests are basically the two coincidence fragments we expected.

Correlations between the kinetic energies of coincident fragments from direct breakup mode of ^{6,7}Li at E_{beam} = 40 MeV are presented in Fig. 7(c),(d). The band-like structures are immediately obvious, which suggests these events have originated true ^{6}Li $\rightarrow \alpha + d$ and ^{7}Li $\rightarrow \alpha + t$ breakup processes. Other breakup events from different modes can also be extracted in the same way.

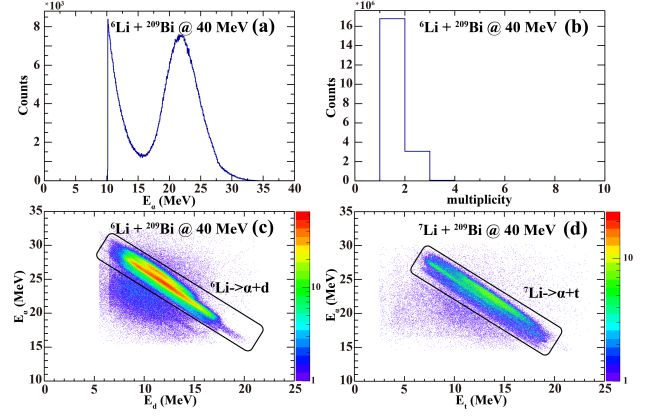Fig. 7. (Color online) (a) Single energy spectrum of inclusive α from No.0-3 telescope units. (b) Particle multiplicity of the entire array. (c)(d) The two-dimensional energy spectrum of the direct breakup modes from ^{6,7}Li at E_{beam} = 40 MeV.

Based on the extracted breakup events, two-body dynamics calculations can be used to reconstruct the breakup reaction Q value to further understand the breakup mechanism. The energy change (Q value) in the reaction was associated with the excitations of the residual target nuclei which can be determined by Eq. (2):

$$Q = E_1 + E_2 + E_{rec} - E_{lab} \tag{2}$$

E_1, E_2 are the kinetic energies for the coincidence particles in the reactions. E_{rec} is the energy of the recoiling target-like nucleus determined by conservation of momentum in three body system. E_{lab} is the laboratory kinetic energy of the incident projectile (E_{beam} for energy loss in the target after correcting).

The reconstructed Q spectra of all breakup modes in the reactions of ^{6,7}Li with ^{209}Bi at E_{beam} = 30, 40 and 47 MeV are shown in Fig. 8, respectively. The Q spectra show the peaks for each excited state of the target-like nucleus, whereas the excitation energy of the target-like nucleus cannot be measured by the detector array directly. In the reaction of ^{6}Li, compared with the direct breakup mode (^{6}Li $\rightarrow \alpha + d$), the breakup of ^{5}Li into $\alpha + p$ after 1n-stripping seems to be the most dominant, as can also be verified in Refs. [22, 26]. Besides, a new breakup mode ^{7}Li $\rightarrow \alpha + t$ was observed for the first time by STARE with obvious Q value peaks. We can observe that the relevance of the ^{7}Li $\rightarrow \alpha + t$ channel increases with the beam energy. The discovery of ^{7}Li $\rightarrow \alpha + t$ breakup mode indicates that the 1n-pickup process cannot be ignored in the reaction of ^{6}Li, which also provides an additional explanation for the origin of inclusive α particles [20, 27].

For the reaction ^{7}Li + ^{209}Bi, the breakup triggered by a 1p-pickup is the most probable channel for ^{7}Li. The breakup after the production of ^{8}Be into two α particles produces multiple peaks in the Q value spectra. However, when the target
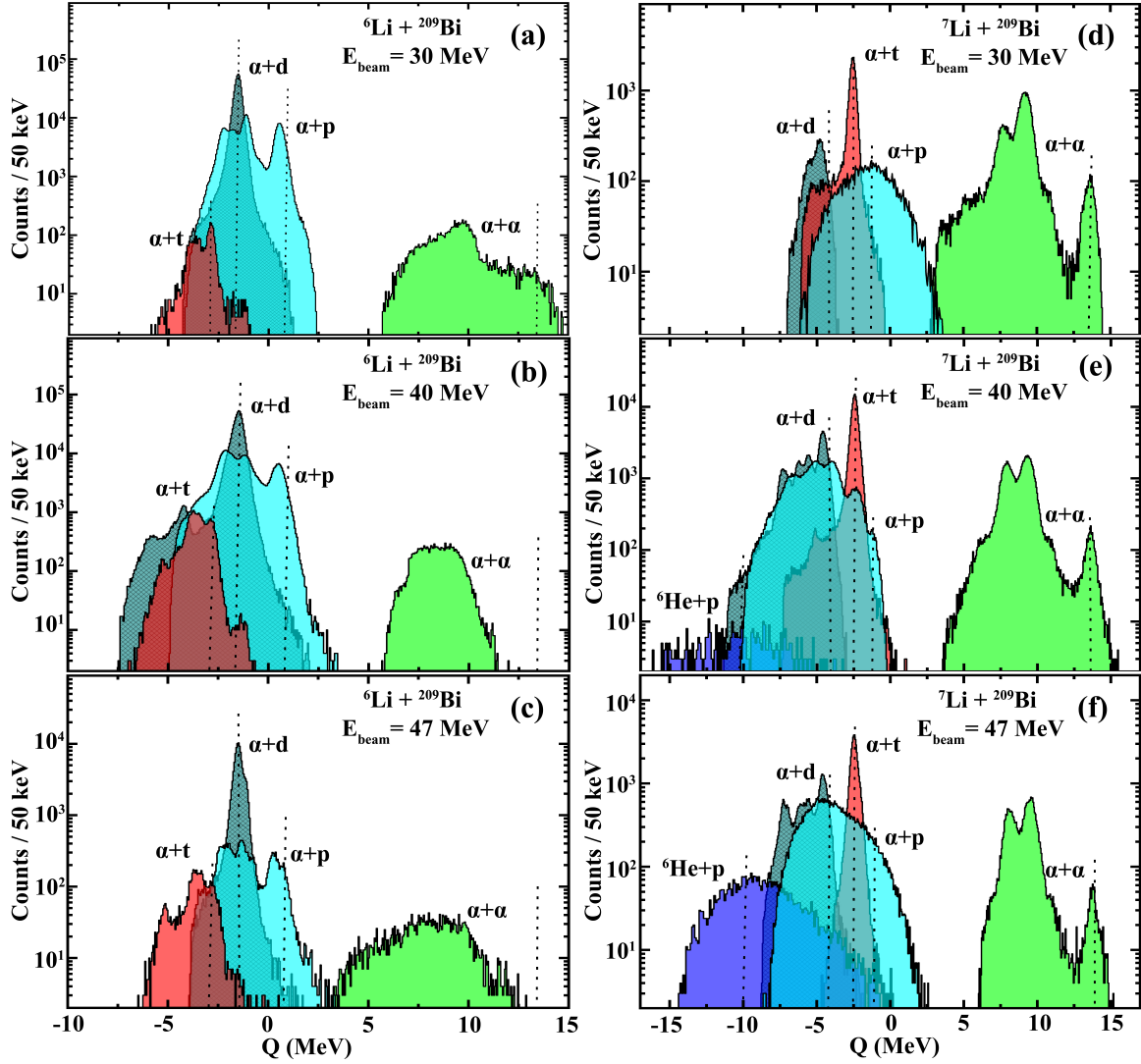
Fig. 8. (Color online) The Q value spectra determined for ^{6,7}Li + ^{209}Bi at E_{beam} = 30, 40, 47 MeV including different breakup modes, the vertical dashed lines indicate the expected Q_{gg} for each breakup mode in reactions of ^{6}Li and ^{7}Li, respectively.

is replaced by a medium-mass nucleus, the conclusion may be inconsistent. In the ^{7}Li + ^{93}Nb system [28], $\alpha + t$ and $\alpha + d$ are obviously dominant. When the beam energy is increased to 40, 47 MeV, despite a very high breakup threshold ($\sim$10 MeV), a significant number of ^{6}He + p events was observed in ^{7}Li + ^{209}Bi system. The present exclusive measurement of ^{6}He in coincidence with a proton that provides direct evidence of the ^{6}He + p cluster configuration of ^{7}Li is very important in understanding the possible nuclear cluster structures of ^{7}Li [29].

V. SUMMARY

In the present work, a new multilayer silicon telescope array was designed and manufactured for the study of the breakup reaction mechanisms induced by weakly bound nuclear systems at energies around the Coulomb barrier. In the new array, the integrated preamplifiers are positioned near the detectors and operate continuously and stably in a low-temperature environment, which is very important for reducing noise. STARE with large solid angle covered greatly improves the coincidence efficiency, making it possible to collect breakup events with very small cross-sections.

STARE has been successfully used to investigate the coincidence measurement of charged fragments in ^{6,7}Li + ^{209}Bi systems at E_{beam} = 30, 40, 47 MeV. Thanks to the powerful particle identification and energy resolution of STARE, different breakup modes can be distinguished clearly by two-body dynamics calculations, along with the observation of new breakup modes.

ACKNOWLEDGMENTS

[1] E. F. Aguilera, P. Amador-Valenzuela, E. Martinez-Quiroz, D. Lizcano, P. Rosales, H. García-Martínez, A. Gómez-Camacho, J. J. Kolata, A. Roberts, L. O. Lamm, G. Rogachev, V. Guimarães, F. D. Becchetti, A. Villano, M. Ojaruega, M. Febbraro, Y. Chen, H. Jiang, P. A. DeYoung, G. F. Peaslee, C. Guess, U. Khadka, J. Brown, J. D. Hinnefeld, L. Acosta, E. S. R. Jr, J. F. P. Huiza, and T. L. Belyaeva, Phys. Rev. Lett. **107**, 092701 (2011).

[2] L. Canto, P. Gomes, R. Donangelo, J. Lubian, and M. Hussein, Physics Reports **596**, 1 (2015), recent developments in fusion and direct reactions with weakly bound nuclei.

[3] N. Takigawa, M. Kuratani, and H. Sagawa, Phys. Rev. C **47**, R2470 (1993).

[4] K. Hagino, A. Vitturi, C. H. Dasso, and S. M. Lenzi, Phys. Rev. C **61**, 037602 (2000).

[5] J. Takahashi, M. Munhoz, E. M. Szanto, N. Carlin, N. Added, A. A. P. Suaide, M. M. de Moura, R. Liguori Neto, A. Szanto de Toledo, and L. F. Canto, Phys. Rev. Lett. **78**, 30 (1997).

[6] J. J. Kolata, V. Guimarães, D. Peterson, P. Santi, R. White-Stevens, P. A. DeYoung, G. F. Peaslee, B. Hughey, B. Atalla, M. Kern, P. L. Jolivette, J. A. Zimmerman, M. Y. Lee, F. D. Becchetti, E. F. Aguilera, E. Martinez-Quiroz, and J. D. Hinnefeld, Phys. Rev. Lett. **81**, 4580 (1998).

[7] M. Trotta, J. L. Sida, N. Alamanos, A. Andreyev, F. Auger, D. L. Balabanski, C. Borcea, N. Coulier, A. Drouart, D. J. C. Durand, G. Georgiev, A. Gillibert, J. D. Hinnefeld, M. Huyse, C. Jouanne, V. Lapoux, A. Lépine, A. Lumbroso, F. Marie, A. Musumarra, G. Neyens, S. Ottini, R. Raabe, S. Ternier, P. Van Duppen, K. Vyvey, C. Volant, and R. Wolski, Phys. Rev. Lett. **84**, 2342 (2000).

[8] C. H. Dasso and A. Vitturi@f, Phys. Rev. C **50**, R12 (1994).

[9] S. B. Moraes, P. R. S. Gomes, J. Lubian, J. J. S. Alves, R. M. Anjos, M. M. Sant'Anna, I. Padrón, C. Muri, R. Liguori Neto, and N. Added, Phys. Rev. C **61**, 064608 (2000).

[10] E. F. Aguilera, J. J. Kolata, F. M. Nunes, F. D. Becchetti, P. A. DeYoung, M. Goupell, V. Guimarães, B. Hughey, M. Y. Lee, D. Lizcano, E. Martinez-Quiroz, A. Nowlin, T. W. O'Donnell, G. F. Peaslee, D. Peterson, P. Santi, and R. White-Stevens, Phys. Rev. Lett. **84**, 5058 (2000).

[11] M. Dasgupta, P. R. S. Gomes, D. J. Hinde, S. B. Moraes, R. M. Anjos, A. C. Berriman, R. D. Butt, N. Carlin, J. Lubian, C. R. Morton, J. O. Newton, and A. Szanto de Toledo, Phys. Rev. C **70**, 024606 (2004).

[12] P. R. S. Gomes, I. Padron, E. Crema, O. A. Capurro, J. O. F. Niello, A. Arazi, G. V. Martí, J. Lubian, M. Trotta, A. J. Pacheco, J. E. Testoni, M. D. Rodríguez, M. E. Ortega, L. C. Chamon, R. M. Anjos, R. Veiga, M. Dasgupta, D. J. Hinde, and K. Hagino, Phys. Rev. C **73**, 064606 (2006).

[13] A. Mukherjee, Subinit Roy, M. Pradhan, M. Saha Sarkar, P. Basu, B. Dasmahapatra, T. Bhattacharya, S. Bhattacharya, S. Basu, A. Chatterjee, V. Tripathi, and S. Kailas, Physics Letters B **636**, 91 (2006).

[14] S. Hu, G. Zhang, G. Zhang, D. Testov, H. Zhang, H. Sun, P. John, J. Valiente-Dobón, Y. Yao, A. Goasduff, M. Siciliano, F. Galtarossa, F. Recchia, D. Mengoni, D. Bazzacco, R. Menegazzo, A. Boso, D. de Angelis, S. Lenzi, D. Napoli, E. Li, and X. Hao, Nuclear Instruments and Methods in Physics Research Section A: Accelerators, Spectrometers, Detectors and Associated Equipment **914**, 64 (2019).

[15] G. Marquínez-Durán, L. Acosta, R. Berjillos, J. Dueñas, J. Labrador, K. Rusek, A. Sánchez-Benítez, and I. Martel, Nuclear Instruments and Methods in Physics Research Section A: Accelerators, Spectrometers, Detectors and Associated Equipment **755**, 69 (2014).

[16] M. Romoli, E. Vardaci, A. Anastasio, C. Boiano, R. Bonetti, F. Cassese, D. Corti, B. D'Aquino, A. DeRosa, P. Di Meo, S. Energico, F. Farinon, T. Glodariu, A. Guglielmetti, G. Inglima, M. La Commara, C. Manea, B. Martin, V. Masone, C. Mazzocchi, M. Mazzocco, Y. Mizoi, M. Nicoletto, L. Parascandolo, P. Parascandolo, D. Pierroutsakou, G. Pontoriere, N. Randazzo, L. Roscilli, M. Sandoli, C. Signorini, V. Sipala, F. Soramel, L. Stroe, M. Valentino, and Y. Watanabe, Nuclear Instruments and Methods in Physics Research Section B: Beam Interactions with Materials and Atoms **266**, 4637 (2008), proceedings of the XVth International Conference on Electromagnetic Isotope Separators and Techniques Related to their Applications.

[17] D. Luong, K. Cook, E. Williams, M. Dasgupta, D. Hinde, R. du Rietz, R. Rafiei, and M. Evers, Proceedings of Science (2012).

[18] Y. Yao, C. Lin, L. Yang, N. Ma, D. Wang, G. Zhang, G. Zhang, H. Jia, F. Yang, F. Zhong, and P. Wen, Chinese Physics C **45** (2021), 10.1088/1674-1137/abe3ee.

[19] Y.-J. Yao, C.-J. Lin, L. Yang, N.-R. Ma, D.-X. Wang, G.-L. Zhang, G.-X. Zhang, H.-M. Jia, and F. Yang, Nuclear Science and Techniques **32**, 14 (2021).

[20] C. Signorini, A. Edifizi, M. Mazzocco, M. Lunardon, D. Fabris, A. Vitturi, P. Scopel, F. Soramel, L. Stroe, G. Prete, E. Fioretto, M. Cinausero, M. Trotta, A. Brondi, R. Moro, G. La Rana, E. Vardaci, A. Ordine, G. Inglima, M. L. Commara, D. Pierroutsakou, M. Romoli, M. Sandoli, A. Diaz-Torres, I. J. Thompson, and Z. H. Liu, Phys. Rev. C **67**, 044607 (2003).

[21] S. Santra, V. Parkar, K. Ramachandran, U. Pal, A. Shrivastava, B. Roy, B. Nayak, A. Chatterjee, R. Choudhury, and S. Kailas, Physics Letters B **677**, 139 (2009).

[22] D. H. Luong, M. Dasgupta, D. J. Hinde, R. du Rietz, R. Rafiei, C. J. Lin, M. Evers, and A. Diaz-Torres, Phys. Rev. C **88**, 034609 (2013).

[23] D. Wang, C. Lin, L. Yang, N. Ma, L.-J. Sun, F. Yang, H. Jia, F.-P. Zhong, and P. Wen, Nuclear Science and Techniques **31** (2020), 10.1007/s41365-020-00755-0.

[24] N. R. Ma, L. Yang, C. J. Lin, H. Yamaguchi, D. X. Wang, L. J. Sun, M. Mazzocco, H. M. Jia, S. Hayakawa, D. Kahl, S. Cha, G. X. Zhang, F. J. Yang, Y. Y. Yang, C. Signorini, Y. Sakaguchi,

K. Abe, M. L. Commara, D. Pierroutsakou, C. Parascandolo, E. Strano, A. Kim, K. Y. Chae, M. Kwag, G. L. Zhang, M. Pan, X. X. Xu, P. W. Wen, F. Zhong, H. H. Sun, and G. qing Guo, The European Physical Journal A **55**, 1 (2019).

[25] "Lise++," (https://lise.frib.msu.edu/lise.html).

[26] D. Luong, M. Dasgupta, D. Hinde, R. du Rietz, R. Rafiei, C. Lin, M. Evers, and A. Diaz-Torres, Physics Letters B **695**, 105 (2011).

[27] S. Santra, S. Kailas, V. V. Parkar, K. Ramachandran, V. Jha, A. Chatterjee, P. K. Rath, and A. Parihari, Phys. Rev. C **85**, 014612 (2012).

[28] S. K. Pandit, A. Shrivastava, K. Mahata, N. Keeley, V. V. Parkar, P. C. Rout, K. Ramachandran, I. Martel, C. S. Palshetkar, A. Kumar, A. Chatterjee, and S. Kailas, Phys. Rev. C **93**, 061602 (2016).

[29] D. Chattopadhyay, S. Santra, A. Pal, A. Kundu, K. Ramachandran, R. Tripathi, B. J. Roy, T. N. Nag, Y. Sawant, B. K. Nayak, A. Saxena, and S. Kailas, Phys. Rev. C **97**, 051601 (2018).